Optical Properties of Anisotropic Polyvalent Metals*

M. J. Kelly†
Victoria University, Wellington, New Zealand

N. W. Ashcroft
Laboratory of Atomic and Solid State Physics, Cornell University, Ithaca, New York 14850

(Received 21 March 1973)

The optical conductivities of single-crystal anisotropic polyvalent metals often exhibit a marked dependence on the polarization of the incident radiation. This can be accounted for straightforwardly by an extension of the second-order theory for the optical response of isotropic systems, and as in the case of the cubic polyvalent metals the expressions for the optical constants can be given in closed form.

I. INTRODUCTION

The marked structure found in the optical conductivities $\sigma(\omega)$ of the cubic polyvalent metals[1-3] (Al is an example) is also a feature of the anisotropic polyvalent metals (Mg, Zn, Cd, Hg, In, etc.). The physical origin of the structure is common to both classes: It is a manifestation of the singular behavior exhibited by the joint density of levels in the (perfect-lattice) single-particle band structure and modified in a relatively minor way by the effects of scattering. In particular, for levels with energies $\mathcal{E}_{n\vec{k}}$ (corresponding to Bloch functions $\psi_{n\vec{k}}$) the quantity $\nabla_{\vec{k}}(\mathcal{E}_{n'\vec{k}} - \mathcal{E}_{n\vec{k}} - \hbar\omega)$ vanishes over a face of the appropriate zone where for direct transitions the bands $\mathcal{E}_{n'\vec{k}}$ and $\mathcal{E}_{n\vec{k}}$ are parallel. For radiation of energy $\hbar\omega$ the calculation of the corresponding $\sigma(\omega)$ can be accomplished using perturbation theory provided that the valence bands of the metals under investigation are reasonably well accounted for by a weak local pseudopotential $U(\vec{r})$. With this restriction in mind, we shall briefly sketch in Sec. II the theory given recently to describe $\sigma(\omega)$ in cubic metals, modifying it where necessary to incorporate changes arising from anisotropy. Transport coefficients are no longer scalar and as a consequence the polarization dependence emerges as a useful probe of the band structure. Scattering effects may be included in a relaxation-time approximation (Sec. III). We also outline the modifications to the sum rules necessary for anisotropic systems. Results are presented for zinc and mercury.

II. DIRECT INTERBAND ABSORPTION

The absorbing power P of an anisotropic metal of volume Ω is

$$P = \Omega \langle \vec{E} \cdot \underline{\sigma}(\omega) \cdot \vec{E} \rangle , \tag{1}$$

where $\underline{\sigma}(\omega)$ is the long-wavelength limit of the frequency-dependent conductivity tensor. If the electric field $\vec{E}$ of the incident light is polarized in the direction $\hat{\epsilon}$, then in the absence of scattering the absorbing power for direct interband excitation processes is[3]

$$P = \Omega E^2 \frac{e^2}{a_0 \hbar} \frac{4\pi}{\hbar\omega} \left(\frac{\hbar^2}{2m}\right)^2 \frac{a_0}{\Omega} \sum_{nn'\vec{k}} f(\mathcal{E}_{n\vec{k}})[1 - f(\mathcal{E}_{n'\vec{k}})]\, \delta(\mathcal{E}_{n'\vec{k}} - \mathcal{E}_{n\vec{k}} - \hbar\omega) \langle \psi_{n'\vec{k}} | \hat{\epsilon} \cdot \vec{\nabla} | \psi_{n\vec{k}} \rangle \langle \psi_{n\vec{k}} | \hat{\epsilon} \cdot \vec{\nabla} | \psi_{n'\vec{k}} \rangle , \tag{2}$$

and the real part of the conductivity tensor is

$$\underline{\sigma}(\omega) = \sigma_a \frac{96\pi^2}{\hbar\omega} \left(\frac{\hbar^2}{2m}\right)^2 \frac{a_0}{\hbar} \sum_{nn'\vec{k}} f(\mathcal{E}_{n\vec{k}})[1 - f(\mathcal{E}_{n'\vec{k}})]\, \delta(\mathcal{E}_{n'\vec{k}} - \mathcal{E}_{n\vec{k}} - \hbar\omega) \langle \psi_{n'\vec{k}} | \vec{\nabla} | \psi_{n\vec{k}} \rangle \langle \psi_{n\vec{k}} | \vec{\nabla} | \psi_{n'\vec{k}} \rangle , \tag{3}$$

where the f's are Fermi occupation factors, and we have separated out a factor $\sigma_a = e^2/24\pi a_0 \hbar$ having the convenient practical value of 5.48×10^{-14} sec^{-1}.

The primary concern here is to account for the location[4] of structure in $\underline{\sigma}(\omega)$ and accordingly it is sufficient in a second-order theory to evaluate the matrix elements appearing in (3) in a two-plane-wave approximation. Let $\vec{K}$ be a reciprocal-lattice vector corresponding to a member of the set of zone planes intersecting the Fermi surface. Denoting the bands in the vicinity of the zone plane by $n = 1$, $n' = 2$ we have

$$\langle \psi_{2\vec{k}} | \vec{\nabla} | \psi_{1\vec{k}} \rangle = \tfrac{1}{2} i \vec{K} (1 + \gamma^2)^{-1/2} ,$$

where

$$\gamma = \frac{\hbar^2}{2m} \frac{k^2 - (\vec{k} - \vec{K})^2}{2U_{\vec{K}}} ,$$

and

$$\Omega U_{\vec{K}} = \int d\vec{r}\, e^{-i\vec{K}\cdot\vec{r}} U(\vec{r}) \tag{4}$$

is the Fourier transform of the (local) periodic pseudopotential. If the crystal contains N cells, each with an N_b atom basis with basis vectors $\vec{\rho}_j$, then

$$U_{\vec{K}} = S_{\vec{K}} V_{\vec{K}},$$

where $V_{\vec{K}}$ is the electron-ion form factor[4] and $S_{\vec{K}}$ is the structure factor per atom:

$$S_{\vec{K}} = N_b^{-1} \sum_{j=1}^{N_b} e^{i\vec{K}\cdot\vec{\rho}_j}.$$

With this notation the reduction of (3) follows the steps leading from Eqs. (7) to (18) of Ref. 3. For a set of equivalent zone planes $\{\vec{K}\}$ we give the result in three parts:

$$\underline{\sigma}(\omega) = \underline{0}, \quad \hbar\omega < 2\,|\,U_{\vec{K}}\,|$$

$$\underline{\sigma}(\omega) = \sigma_a(a_0K)\left|\frac{2U_K}{\hbar\omega}\right|^2\left(1-\left|\frac{2U_K}{\hbar\omega}\right|^2\right)^{-1/2}\sum_{\{\vec{K}\}} 3\hat{K}\hat{K}, \quad |\,2U_K\,| < \hbar\omega < \hbar\omega_0$$

$$\underline{\sigma}(\omega) = \sigma_a(a_0K)\left|\frac{2U_K}{\hbar\omega}\right|^2\left(1-\left|\frac{2U_K}{\hbar\omega}\right|^2\right)^{-1/2} \times \frac{(\hbar\omega+\hbar\omega_0)(\hbar\omega_1-\hbar\omega)}{4\mathcal{E}_K\hbar\omega}\sum_{\{\vec{K}\}} 3\hat{K}\hat{K}, \quad \hbar\omega_0 < \hbar\omega < \hbar\omega_1 \tag{5}$$

where $\hat{K} = \vec{K}/K$ and $\mathcal{E}_{\vec{K}} = \hbar^2K^2/2m$. In Eqs. (5), the frequencies $\hbar\omega_0$ and $\hbar\omega$ are defined[3], respectively, by

$$\hbar\omega_0 = 2(\mathcal{E}_K\mathcal{E}_F + |\,U_K\,|^2)^{1/2} - \mathcal{E}_K = \hbar\omega_1 - 2\mathcal{E}_K,$$

where $\mathcal{E}_F$ is the Fermi energy.

The anisotropy of the conductivity is apparent in the factor $\sum_{\{\vec{K}\}} 3\hat{K}\hat{K}$ (which reduces, in a cubic system, to a unit matrix weighted by the membership of the set). It is constructed from those equivalent reciprocal-lattice vectors whose associated zone planes form the zones of interest in the optical problem (for example, planes which cut the Fermi surface). In this context we will refer to $\underline{T}(\vec{K}) = \sum_{\{\vec{K}\}} 3\hat{K}\hat{K}$ as a zone tensor. The zone tensors clearly depend on structure but are all symmetric.

III. SCATTERING, OPTICAL MASSES, AND SUM RULES

Interband scattering effects are incorporated by introducing a phenomenological relaxation time τ and replacing (3) for the two-band model by[5]

$$\underline{\sigma}(\omega) = \sigma_a \frac{96\pi}{i\hbar\omega}\left(\frac{\hbar^2}{2m}\right)^2 \frac{a_0}{\Omega}\sum_{\vec{k}}\left(\frac{\hbar\omega}{\mathcal{E}_{2\vec{k}}-\mathcal{E}_{1\vec{k}}}\right)^2 \times\left(\frac{\langle\psi_{2\vec{k}}\,|\,\vec{\nabla}\,|\,\psi_{1\vec{k}}\rangle\langle\psi_{1\vec{k}}\,|\,\vec{\nabla}\,|\,\psi_{2\vec{k}}\rangle}{\mathcal{E}_{2\vec{k}}-\mathcal{E}_{1\vec{k}}-\hbar(\omega+i/\tau)} + \frac{\langle\psi_{1\vec{k}}\,|\,\vec{\nabla}\,|\,\psi_{2\vec{k}}\rangle\langle\psi_{2\vec{k}}\,|\,\vec{\nabla}\,|\,\psi_{1\vec{k}}\rangle}{\mathcal{E}_{2\vec{k}}-\mathcal{E}_{1\vec{k}}+\hbar(\omega+i/\tau)}\right), \tag{6}$$

the sum being taken over those $\vec{k}$ for which the lower band is filled and the upper is empty. It is clear from the structure of Eq. (6) that the contributions from equivalent planes will continue to incorporate $\underline{T}$ as a linear factor. Accordingly the results of Secs. III and IV of Ref. 3 can be taken over completely by simply including the appropriate zone tensor $\underline{T}$ for a given set of equivalent planes.

For a cubic metal the inverse optical mass can be taken as a scalar. In an anisotropic system we are led to an inverse-optical-mass tensor

$$\left(\frac{m}{m_{\rm opt}}\right)_{ij} = \frac{m}{4\pi^3 n_e\hbar^2}\sum_n \int d\vec{k}\,\frac{\partial^2\mathcal{E}_{n\vec{k}}}{\partial k_i\partial k_j}, \tag{7}$$

where the integral is taken over the occupied states, n_e being the conduction-electron density. The two-band model gives immediately

$$\frac{\partial^2\mathcal{E}_{n\vec{k}}}{\partial k_i\partial k_j} = \frac{\hbar^2}{m}\delta_{ij} \pm \frac{\mathcal{E}_K}{|\,U_{\vec{K}}\,|}\frac{\hbar^2}{2m}(1+\gamma^2)^{-3/2}\hat{K}_i\hat{K}_j, \tag{8}$$

where the positive sign is associated with the upper band ($n = 2$), and the negative with the lower ($n = 1$). Integration over the occupied levels then gives (for all contributing planes $\{\vec{K}\}$)

$$\delta_{ij} - \left(\frac{m}{m_{\rm opt}}\right)_{ij} = \frac{1}{4}\sum_{\{K\}}\frac{K}{2k_F}\left(\frac{2\,|\,U_K\,|}{\mathcal{E}_F}\int_1^{x_0}\frac{dx}{x(x^2-1)^{1/2}} + \frac{|\,U_K\,|^2}{\mathcal{E}_F\mathcal{E}_K}\int_{x_0}^{x_1}\frac{(x+z_0)(z_1-x)}{x^2(x^2-1)^{1/2}}\,dx\right)3\hat{K}_i\hat{K}_j \tag{9}$$

with $z_\alpha = \hbar\omega_\alpha/2\,|\,U_K\,|$.

Equation (9) may also be examined in the light of the conductivity sum rule. If n_e is the conduction-electron density, then for the total transverse conductivity we have[6]

$$(2/\pi)\int_0^\infty \mathrm{Re}\sigma_{ij}(\omega)\,d\omega = (n_e e^2/m)\,\delta_{ij}, \tag{10}$$

which implies that the oscillator strength appearing in the direct interband absorption is removed from the intraband (Drude) absorption. The latter is calculated (as in Ref. 3) with the appropriate optical mass given by Eq. (9).

IV. RESULTS AND DISCUSSION

There is a scarcity of published optical data for single-crystal anisotropic metals and frequently significant disagreement[7] between the sets of optical conductivities derived for a given metal. Much of the primary data is in the form of polarization-dependent reflectivities and it is therefore con-

venient to present the theoretical results also in terms of reflectivities, the latter being readily derived from $\underline{\sigma}(\omega)$. With only a minor loss in accuracy the computational aspects of the analysis can be greatly simplified by the use of the infinite-relaxation-time limit of the imaginary part of the conductivity. Although this differs somewhat from the results expected from $\mathrm{Im}\underline{\sigma}$ given by Eq. (6), the deviations are mostly at higher energies and do not affect the conclusions. It is also worth noting at this point that although $\underline{\sigma}(\omega)$ given by Eq. (5) is continuous, its derivative at $\hbar\omega_0$ exhibits a small discontinuity[8] reflecting the point at which filled levels in the second band cease to inhibit direct transitions. The resulting structure, particularly in $\mathrm{Im}\underline{\sigma}$, is weak and largely eliminated by the use of the computationally more cumbersome form of $\mathrm{Im}\underline{\sigma}$ given by Eq. (6).

A. Hexagonal Systems

The zone tensors $\underline{T}$ for hexagonal metals are entirely diagonal: Choosing the z axis to be parallel to the c axis they have the form

$$\underline{T}(\vec{K}) = \begin{pmatrix} a(\vec{K}) & 0 & 0 \\ 0 & a(\vec{K}) & 0 \\ 0 & 0 & b(\vec{K}) \end{pmatrix} . \qquad (11)$$

Since the absorption is proportional to $\sum_{ij} \hat{\epsilon}_i \sigma_{ij} \hat{\epsilon}_j$, the experimentally observed anisotropy of the optical properties of Mg, Cd, and Zn, for example, is easily accounted for. In each of these three metals, three sets of zone planes feature prominently in the interband absorption structure. These are the six planes parallel to the c axis in the first Brillouin zone and the boundary planes of the Jones zone.[9] In most cases the sloping planes of the latter dominate the optical absorption.

Rubloff[10] has given results for the optical properties of Zn which, from the point of view of the present considerations, are in a convenient form. In Fig. 1 we show the best over-all fit to the data achieved by using $|U_{\vec{K}}|$ and τ as adjustable parameters. The assignment of the $|U_{\vec{K}}|$ appears to be unambiguous, and, in particular, the fact that $|U_{10\bar{1}0}| \approx 0$ indicates why virtually no structure arises from the six equivalent first-zone faces in the $\hat{\epsilon} \perp \vec{c}$ optical conductivity. Note that the form factor corresponding to the data implies a value of $q_0/2k_F$ [where $U(q_0) = 0$] equal to 0.85 in agreement with the Heine-Abarenkov model potential[11] but the slope of the form factor in this region is a little greater.

As was found in Ref. 3, the value of τ partly determines the widths of the absorption peaks and, hence, the drop in reflectivity. Its value is comparable to that expected from a Drude analysis of

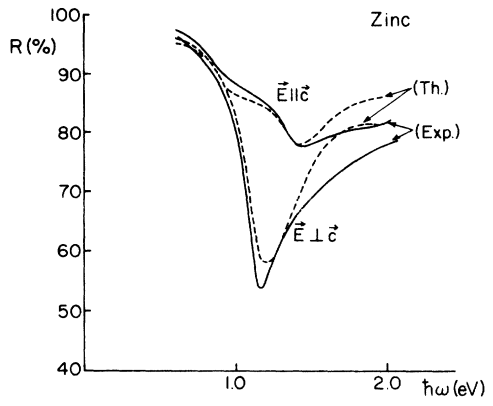

FIG. 1. Polarization dependent reflectivities from zinc. The experimental results (full line) are those of Rubloff (Ref. 10). The calculated curves (dashed lines) correspond to the choice $|U_{10\bar{1}0}| = 0.0$ eV, $|U_{0002}| = 0.485$ eV, $|U_{10\bar{1}1}| = 0.74$ eV, and $\tau = 0.4 \times 10^{-14}$ sec.

the static conductivity. The inverse-optical-mass tensor in Zn is diagonal and has components 0.52, 0.52, and 0.62. For both polarizations we expect (as a consequence) more than half of the absorption to originate from intraband (Drude) processes, a conclusion somewhat different from Rubloff's. Optical masses derived from extrapolation of the reflectivity curve below the lower limit of experimental observation are, however, quite sensitive to the details of the continuation.

It is worth pointing out that for many of the reasons that Al is often thought to be an ideal simple metal in the class of cubic metals, Mg is the anisotropic counterpart. Although published reflectivity data on Mg is sparse, the optical conductivity and its dependence on polarization should be amenable to interpretation within the weak-potential model.[12]

B. Rhombohedral Systems

By taking the pole to be along the trigonal axis, the zone tensors $\underline{T}$ of the rhombohedral system take the form

$$\underline{T}(\vec{K}) = \begin{pmatrix} a(\vec{K}) & 0 & 0 \\ 0 & a(\vec{K}) & 0 \\ 0 & 0 & b(\vec{K}) \end{pmatrix} .$$

In the case of divalent mercury (in its α-phase), the Fermi energy appears to be above the band gap at six of the faces of its zone[13] (i.e., those containing the point L) and below the gap on the remaining eight. The absorption associated with the latter will exhibit no edges and the optical conductivity will be dominated (in the range of interest) by the L-face contributions.

The reported optical data on a Hg single crystal[14] are incomplete to the extent that the orientation

of the sample was not determined. The sensitivity to orientation of the optical data can be gauged from Fig. 2, where we show the polarization dependence of the calculated reflectivity for $\hat{\epsilon}$ parallel to ΓX, ΓZ (the trigonal axis), and ΓL. The extent of the variation precludes a fine determination of the band gaps and the relaxation time, and we have attempted to reproduce only the main dip in reflectivity assuming that the light was normally incident on an L face. The value obtained for the corresponding pseudopotential coefficient of 0.95 eV is slightly larger than the de Haas–van Alphen result of Brandt and Rayne.[15] Chokye *et al.* achieved a partial analysis of their data by assuming a cubic crystal structure for mercury. The calculations that produced the results summarized in Fig. 2 yield an inverse optical mass tensor of

$$\begin{pmatrix} 0.403 & 0 & 0 \\ 0 & 0.403 & 0 \\ 0 & 0 & 0.409 \end{pmatrix}.$$

The leading pair of entries on the diagonal are equal, of course, by symmetry. That the third is almost the same is somewhat fortuitous. The integrated total absorption required to evaluate the tensor includes the contributions from the eight faces exhibiting solely normal interband absorption which extends to somewhat higher energies than the contributions from the six parallel-band faces. The six faces contribute mainly to the 11 and 22 components, while the eight faces contribute mainly to the 33 component.

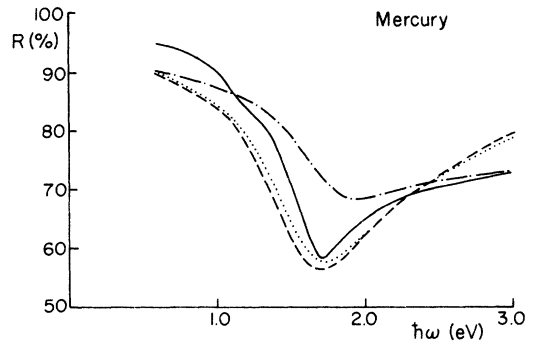

FIG. 2. Polarization-dependent reflectivities from mercury. The experimental results (full line) are those of Choyke *et al.* (Ref. 14). The calculated curves correspond to the choice $|U_{011}| = 0.95$ eV, $|U_{110}| = 0.66$ eV, and $|U_{111}| = 0.66$ eV, and $\tau = 0.15 \times 10^{-14}$ sec. Polarization directions are (---) $\hat{\epsilon} = [100]$ (along ΓX in the zone); (• • •) $\hat{\epsilon} = [001]$ (along ΓZ); and (-• -• -•) $\hat{\epsilon} = [0.912, 0, 0.410]$ (along ΓL).

These examples illustrate that the present analysis may be used quite straightforwardly for those metals where the two-band approximation adequately represents their band structure near zone faces. A further requirement is that the upper of the bands be at least partially occupied.

ACKNOWLEDGMENTS

One of us (N. W. A.) wishes to thank the Departments of Mathematics and Physics at Victoria University, Wellington, for their kind hospitality.

*Work supported in part by the National Science Foundation under Grant No. GP27355, and in part by the National Science Foundation, Grant No. GH33637 through the facilities of the Materials Science Center of Cornell University, MSC No. 1934.

†Present address: Cavendish Laboratory, Cambridge, England.

[1]G. P. Motulevich, Usp. Fiz. Nauk **97**, 211 (1969) [Sov. Phys.-Usp. **12**, 80 (1969)].

[2]W. A. Harrison, Phys. Rev. **147**, 467 (1966).

[3]N. W. Ashcroft and K. Sturm, Phys. Rev. B **3**, 1898 (1971).

[4]The oscillator strengths are given correctly only when the real (rather than pseudo) Bloch functions are used. For the present purpose it is permissible to ignore the small frequency-dependent correction arising from the use of both the pseudopotential and pseudo-wave-functions.

[5]H. Ehrenreich, in *Optical Properties of Solids*, edited by J. Tauc (Academic, New York, 1966); H. Ehrenreich and M. H. Cohen, Phys. Rev. **115**, 786 (1959); S. J. Adler, Phys. Rev. **126**, 413 (1962); H. Ehrenreich and H. R. Philipp, Phys. Rev. **128**, 1622 (1962). The replacement of ω by $\omega + i/\tau$ in the collisionless expression for the optical conductivity appears to imply (if number is to be conserved) that the chemical potential assumes a small spatially varying component. The modification resulting for a single parabolic band has been given by N. D. Mermin, Phys. Rev. B **1**, 2362 (1970).

[6]R. Kubo, J. Phys. Soc. Jap. **12**, 570 (1957); P. C. Martin, Phys. Rev. **161**, 143 (1967).

[7]These have been attributed in part to experimental difficulties (see, for example, I. Yu. Rapp and R. G. Yarovaya, Fiz. Tverd. Tela **11**, 516 (1969) [Sov. Phys.-Solid State **11**, 412 (1969)].

[8]It is straightforward to show from Eqs. (10) and (13) of Ref. 3 that for cubic systems the change in the logarithmic derivative of the real part of $\sigma(\omega)$ at ω_0 is $\Delta(\partial \ln \sigma(\omega)/\partial \ln \omega)_{\omega=\omega_0} = (1/2)(1 + \hbar\omega_0/\epsilon_K)$, which therefore gives an independent experimental measurement of ϵ_K.

[9]Details of the zone structure can be found in H. Jones, *Theory of Brillouin Zones* (North-Holland, Amsterdam, 1960), p. 192.

[10]G. W. Rubloff, Phys. Rev. B **3**, 285 (1971).

[11]These are summarized in the review article by M. L. Cohen and V. Heine, Solid State Phys. **24**, 38 (1970).

[12]Data are also available on Cd [R. J. Bartlett, D. W. Lynch, and R. Rosei, Phys. Rev. B **3**, 4074 (1971)] and it appears here that the Fermi level may lie in the band gap at the $(10\bar{1}0)$ face, implying that $|\hbar\omega_0/2U_K| < 1$ here. In the context of optical absorption the effects of these bands are much more akin to those in the alkali metals.

[13]Reference 9, p. 58.

[14]W. J. Choyke, S. H. Vosko, and T. W. O'Keefe, Solid State Commun. **9**, 361 (1971).

[15]G. B. Brandt and J. A. Rayne, Phys. Rev. **148**, 653 (1966).